

EKF-Based Speed Sensorless Direct Torque Control of Induction Motor Drives

Sebti Belkacem, Farid Nacéri and Rachid Abdessemed
 Leb Research Laboratory, University of Batna, Algeria

Abstract: This study presents a robust sensorless Direct Torque Control (DTC) method for Induction Motor (IM) for estimation of stator flux components and rotor speed based on The Extended Kalman Filter (EKF). The model of IM and its EKF models in Matlab/Simulink simulation environment are developed. The proposed EKF speed and flux estimation method is also proved insensitive to the IM parameter variations. Simulation results demonstrate a good performance and robustness.

Key words: DTC, Extended Kalman Filter (EKF), IM, sensorless control, anti-windup PI

INTRODUCTION

In recent years, several studies have been developed which propose alternative solutions to the FOC control of a PWM inverter-fed motor drive with two objectives: first, achievement of an accurate and fast response of the flux and the torque and second, reduction in the complexity of the control system. Among the various proposals, Direct Torque and Flux Control (DTFC) also called Direct Torque Control (DTC), has found wide acceptance, (Bottiglieri *et al.*, 2003).

Since its introduction in 1985, the Direct Torque Control (DTC) (Takahashi and Noguchi, 1986), principle was widely used for IM drives with fast dynamics. Despite its simplicity, DTC is able to produce very fast torque and flux control, if the torque and the flux are correctly estimated, is robust with respect to motor parameters and perturbations. As it is well known, speed sensors like tachometers or incremental encoders increase the size and the cost of systems unnecessarily. Similar problems arise with the addition of search coils or Hall Effect sensors to the motor for the measurement of flux, hindering functionality in terms of implementation. Thus, to improve the overall system performance, state estimators or observers are usually more preferable than physical measurements, (Belkacem *et al.*, 2005; Akin, 2003; Barut, 2005; Chavez and Velazquez, 2004; Belkacem *et al.*, 2005).

The objectives of sensorless drives control are:

- Reduction of hardware complexity and cost,
- Increased mechanical robustness,
- Operation in hostile environments,
- Higher reliability,
- Unaffected machine inertia.

The Extended Kalman Filter is an optimal stochastic observer in the least-square sense for estimating the states of dynamic non-linear systems and provides optimal filtering of the noises in measurement and inside the system if the covariances of these noises are known. Hence it is a viable candidate for the on-line determination of the speed of IM, EKF is considered to be suitable for use in high-performance induction motor drives and it can provide accurate speed estimates in a wide speed-range, including very low speed and seem to be between the most promising methods thanks to their good performance. They have the advantage to provide both flux and mechanical speed estimates without problems of open-loop integration.

For the speed regulation, the saturation of the manipulated variable can involve a phenomenon of racing of the integral action during the great variations (starting of the machine), which is likely to deteriorate the performances of the system or even to destabilize it completely, the solution consists in correcting the integral action.

The contribution of this study is the development of an EKF based speed sensorless DTC system for an improved performance, the especially against variations in the load torque. The developed EKF algorithm involves the estimation of speed and stator flux. The performance of the control system with the proposed EKF algorithm has been demonstrated with simulations using Matlab/Simulink.

MODELING OF THE INDUCTION MOTOR

The space-state equations of the induction motor can be written as:

$$\begin{cases} \dot{x} = Ax + BU \\ y = Cx \end{cases} \quad (1)$$

Where:

$$x = \begin{bmatrix} i_{sa} & i_{sb} & \Psi_{ra} & \Psi_{rb} \end{bmatrix}^T$$

$$U = \begin{bmatrix} V_{sa} & V_{sb} \end{bmatrix}^T, y = \begin{bmatrix} i_{sa} & i_{sb} \end{bmatrix}^T$$

$$A = \begin{bmatrix} -\gamma & 0 & \frac{K}{T_r} & K\omega_r \\ 0 & -\gamma & -K\omega_r & \frac{K}{T_r} \\ \frac{M}{T_r} & 0 & -\frac{K}{T_r} & -\omega_r \\ 0 & \frac{M}{T_r} & \omega_r & -\frac{K}{T_r} \end{bmatrix}, B = \begin{bmatrix} \frac{1}{\sigma L_s} & 0 \\ 0 & \frac{1}{\sigma L_s} \\ 0 & 0 \\ 0 & 0 \end{bmatrix}$$

$$C = \begin{bmatrix} 1 & 0 & 0 & 0 \\ 0 & 1 & 0 & 0 \end{bmatrix}^T, K = \begin{bmatrix} M \\ \sigma L_s L_r \end{bmatrix}, \gamma = \left[\frac{R_s}{\sigma L_s} + \frac{R_r M^2}{L_r^2 \sigma L_s} \right]$$

Principle of the DTC: DTC is a control philosophy exploiting the torque and flux producing capabilities of ac machines when fed by a voltage source inverter that does not require current regulator loops, still attaining similar performance to that obtained from a vector control drive.

Behavior of stator flux: In the reference (α, β) , the stator flux can be obtained by the following equation:

$$\bar{V}_s = R_s \bar{I}_s + \frac{d}{dt} \bar{\Psi}_s \quad (2)$$

By neglecting the voltage drop due to the resistance of the stator to simplify the study (for high speeds), we find:

$$\bar{\Psi}_s \approx \bar{\Psi}_{s0} + \int_0^t \bar{V}_s dt \quad (3)$$

For one period of sampling, the voltage vector applied to the asynchronous machine remains constant, we can write:

$$\bar{\Psi}_s(k+1) \approx \bar{\Psi}_s(k) + \bar{V}_s T_e \quad (4)$$

Table 1: Selection table for direct torque control

$\Delta \Psi_s$	ΔC^*	S ¹	S ²	S ³	S ⁴	S ⁵	S ⁶
1	1	V ²	V ³	V ⁴	V ⁵	V ⁶	V ¹
	0	V ⁷	V ⁰	V ⁷	V ⁰	V ⁷	V ⁰
	-1	V ⁶	V ¹	V ²	V ³	V ⁴	V ⁵
0	1	V ³	V ⁴	V ⁵	V ⁶	V ¹	V ²
	0	V ⁰	V ⁷	V ⁰	V ⁷	V ⁰	V ⁷
	-1	V ⁵	V ⁶	V ¹	V ²	V ³	V ⁴

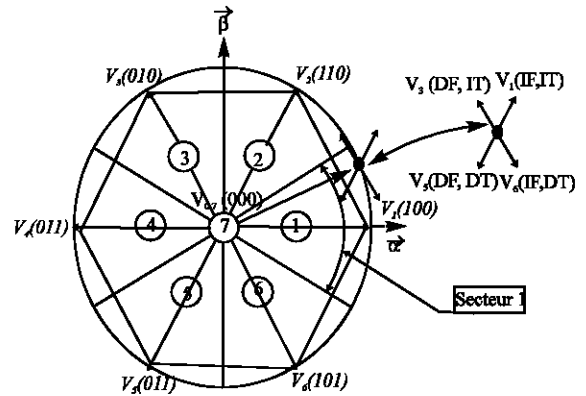


Fig. 1: Partition of the complex plan in six angular sectors

Behavior of the torque: The electromagnetic torque is proportional to the vector product between the stator and rotor flux according to the following expression:

$$C_e = k(\bar{\Psi}_s \times \bar{\Psi}_r) = k |\bar{\Psi}_s| |\bar{\Psi}_r| \sin(\delta) \quad (5)$$

Development of the commutation strategy: Table 1, shows the commutation strategy suggested by Takahashi and Noguchi (1986) to control the stator flux and the electromagnetic torque of the IM.

The Fig. 1 gives the partition of the complex plan in six angular sectors $S_{j=1...6}$.

It : Increase the torque, DT: Decrease the torque

IF : Increase the flux DF: Decrease the flux

DEVELOPMENT OF THE EKF ALGORITHM

The Kalman filter is a well-known recursive algorithm that takes the stochastic state space model of the system together with measured outputs to achieve the optimal estimation of states (Leite *et al.*, 2004; a,b; Barut *et al.*, 2003; Sensorless Control, 1997). The optimality of the state estimation is achieved with the minimization of the mean estimation error. EKF, is used for the estimation of

$$\hat{I}_{s\alpha}, \hat{I}_{s\beta}, \bar{\Psi}_{sa}, \bar{\Psi}_{s\beta} \text{ and } \omega_r$$

and $W\hat{\omega}_r$ (Fig. 2).

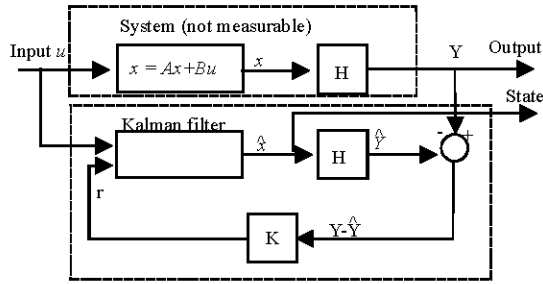


Fig. 2: Shows the structure of a kalman filter

Table 2: Im parameters

P = 4 KW	f = 50 Hz	W _r = 1440 rpm	V _r = 380 V
R _s = 1.2 Ω	R _r = 1.8 Ω	L _s = 0.1554 H	L _r = 0.1568 H
T _r = 0.0871 s	M = 0.15 H	J = 0.07 kgm ²	P = 2

The discrete model of the IM can be given as follows:

$$\begin{cases} \dot{x}(k) = f(x(k), u(k), k) + G(k)w(k) \\ y(k) = h(x(k), k) + v(k) \end{cases} \quad (6)$$

With: Is the measurement noise and v (k): Is the process noise and (Table 2).

APPLICATION OF THE EXTENDED KALMAN FILTER

The speed estimation algorithm of the extended Kalman filter can be simulated by the Matlab/Simulink software, which consists of an S-Function block as shown in Fig. 3.

Prediction of the state vector: Prediction of the state vector at sampling time (k+1), from the input u (k), state vector at previous sampling time.X(K/K)

$$\hat{x}(k+1/k) \hat{=} F(\hat{x}(k/k), u(k)) \quad (7)$$

Where:

$$F = \begin{bmatrix} (1-T_s\gamma)i_{sa} + T_s \frac{MR_r}{L_r^2 K} \psi_{ra} + T_s \frac{M\omega_r}{L_r K} \psi_{rb} + T_s \frac{1}{K} V_{sa} \\ (1-T_s\gamma)i_{sb} - T_s \frac{M\omega_r}{L_r K} \psi_{ra} + T_s \frac{MR_r}{L_r^2 K} \psi_{rb} + T_s \frac{1}{K} V_{sb} \\ T_s \frac{M}{T_r} i_{sa} + \left(1 - T_s \frac{1}{T_r}\right) \psi_{ra} - T_s \omega_r \psi_{rb} \\ T_s \frac{M}{T_r} i_{sb} + T_s \omega_r \psi_{ra} + \left(1 - T_s \frac{1}{T_r}\right) \psi_{rb} \\ w_r \end{bmatrix}$$

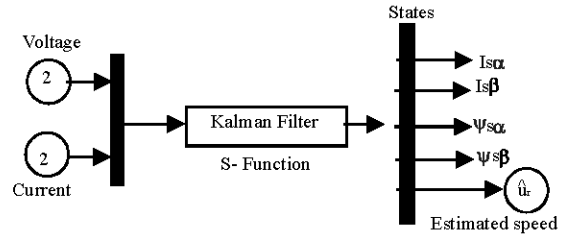


Fig. 3: Simulink model of EKF speed estimation

Prediction covariance computation: The prediction covariance is updated by:

$$P(k+1/k) = F(k)P(k)F(k)^T + Q \quad (8)$$

Where:

Q: Covariance matrix of the system noise

$$F(k) = \left. \frac{\partial f}{\partial x} \right|_{x(k)=\hat{x}(k/k)} \quad (9)$$

With:

$$\frac{\partial F}{\partial x} = \begin{bmatrix} 1-T_s\gamma & 0 & T_s \frac{MR_r}{L_r^2 K} & T_s \frac{M\omega_r}{L_r K} & T_s \frac{M}{L_r K} \psi_{rb} \\ 0 & 1-T_s\gamma & -T_s \frac{M\omega_r}{L_r K} & T_s \frac{MR_r}{L_r^2 K} & -T_s \frac{M}{L_r K} \psi_{ra} \\ T_s \frac{M}{T_r} & 0 & 1-T_s \frac{1}{T_r} & T_s \omega_r & T_s \psi_{rb} \\ 0 & T_s \frac{M}{T_r} & T_s \omega_r & 1-T_s \frac{1}{T_r} & T_s \psi_{ra} \\ 0 & 0 & 0 & 0 & 1 \end{bmatrix}$$

$$\frac{\partial h}{\partial x} = \begin{bmatrix} 1 & 0 & 0 & 0 & 0 \\ 0 & 1 & 0 & 0 & 0 \end{bmatrix} \quad (10)$$

Kalman gain computation: The Kalman filter gain (correction matrix) is computed as:

$$L(k+1) = P(k+1/k).C(k)^T . \quad (11)$$

$$(C(k)P(k+1/k)C(k)^T + R)^{-1}$$

With:

$$C(k) = \left. \frac{\partial c(x(k))}{\partial x(k)} \right|_{x(k)=\hat{x}(k)} \quad (12)$$

State vector estimation: The predicted state-vector is added to the innovation term multiplied by Kalman gain to compute state-estimation vector. The state-vector estimation (filtering) at time (k) is determined as:

$$\hat{x}(k+1/k+1) = \hat{x}(k+1/k) + L(k+1)(y(k+1) - C\hat{x}(k+1/k))$$

DETERMINATION OF THE NOISE AND STATE COVARIANCE MATRICES

The goal of the Kalman filter is to obtain unmeasurable states (i.e., covariance matrices Q, R, P of the system noise vector, measurement noise vector and system state vector (x) respectively). In general, by means of noise inputs, it is possible to take computational inaccuracies, modelling errors and errors in measurements into account in modelling the system. The filter estimation (\hat{x}) is obtained from the predicted values of the states (x) and this is corrected recursively by using a correction

term, which is product of the Kalman gain (L) and the deviation of the estimated measurement output vector and the actual output vector ((y - C \hat{x})). The system noise covariance matrix (Q) is [5×5], and the measurement noise covariance matrix (R) is [2×2] matrix, Q and R are diagonal, and only 5 elements must be known in Q and 2 elements in R.

SYSTEM OF SPEED REGULATION

The saturation of the manipulated variable can involve a phenomenon of racing of the integral action during the great variations (starting of the machine), which is likely to deteriorate the performances of the system or even to destabilize it completely. To overcome this phenomenon, a solution consists in correcting the integral action according to the diagram of Fig. 4 (Coa *et al.*, 2002; Zaccarian and Teal, 2004).

The stator flux is a function of the rotor flux which represented by:

$$\begin{cases} \psi_{sa} = \sigma L_s i_{sa} + \frac{M}{L_r} \psi_{ra} \\ \psi_{sb} = \sigma L_s i_{sb} + \frac{M}{L_r} \psi_{rb} \end{cases} \quad (13)$$

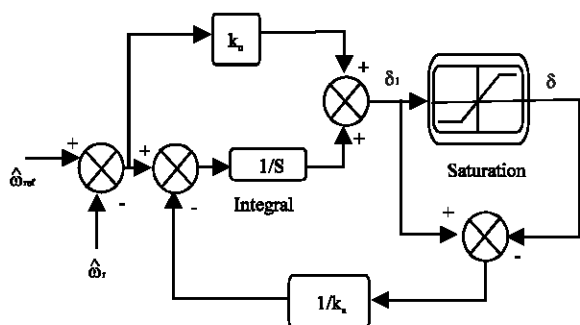


Fig. 4: Structure of the anti-windup PI system

PROPOSED SENSORLESS IM DRIVE

The proposed sensorless IM drive is shown in Fig. 5. The drive operates at constant stator flux uses DTC to provide torque control. The speed controller

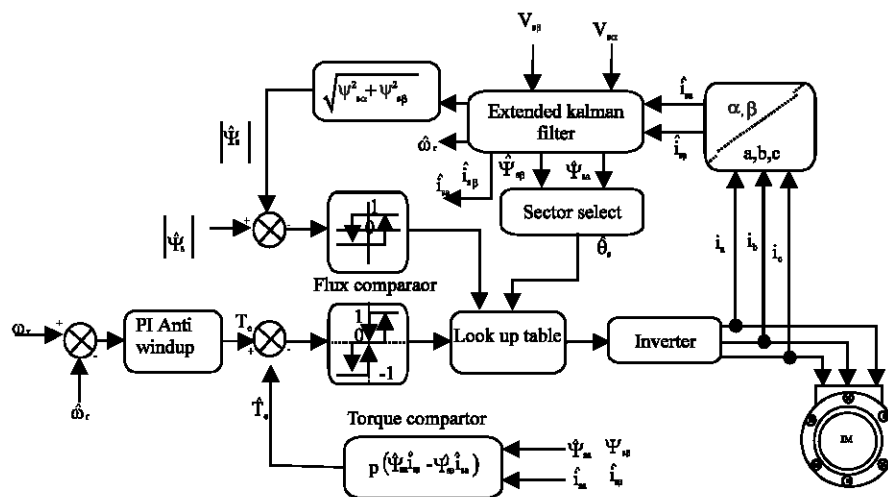


Fig. 5: Speed sensorless direct torque control system using extended kalman filter

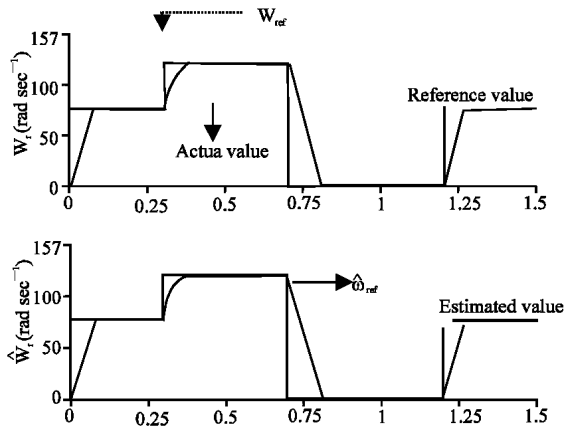


Fig. 6: Reference actual and estimated speed

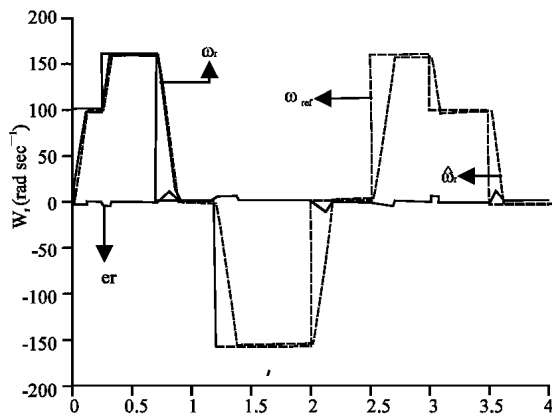


Fig. 7: High speed no-load, four quadrant speed estimation with EKF

is an anti-windup PI regulator that generates the reference torque. The stator flux is estimated by the EKF and used in the DTC control.

RESULTS AND DISCUSSION

The sensorless IM drive of Fig. 5 was verified using simulations. In order to show the performances and the robustness of the EKF algorithm, we simulated different cases, which are presented thereafter. The static and dynamic performances of the EKF are analyzed according to the simulation of the following transients:

Comparison on the level of the regulation speed: Figure 6 presents the actual, estimated speeds, respectively. The estimated speed follows the real speed.

Inversion of the speed: To test the robustness of the system, we applied a changing of the speed reference from 157 rad sec⁻¹ to -157 rad sec⁻¹ at t=1.2s. Figure 7

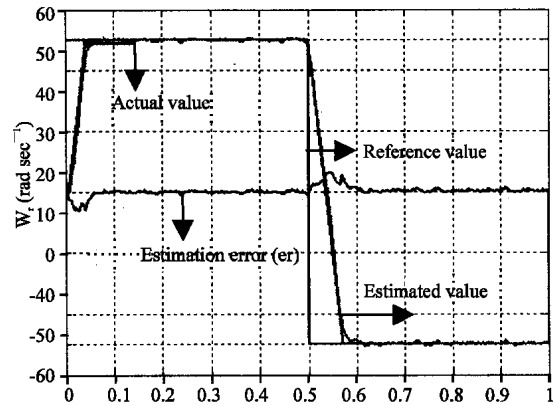


Fig. 8: Low speed actual estimated and estimation error

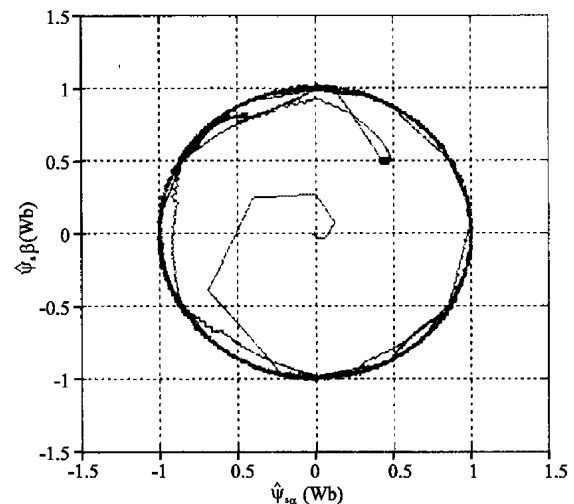


Fig. 9: Trajectory of the estimated stator flux components

presents the actual, estimated speeds, respectively and the estimation error (er). The estimation algorithm is robust because the variation of the speed is important and the estimated speed follows the real speed when the motor starts and at the moment of speed inversion.

Operation at low speed : To test the speed estimation, simulation was established in low speed. Figure 8. Illustrate simulation results of the process of speed estimation with a speed reference equal $W_{ref} = 50$ (rad sec⁻¹). We can see that the speed follow perfectly the speed reference however

Figure 9 illustrates the trajectory of the estimated stator flux; the deviation detected is caused by the instantaneous reversal of the speed at the zero crossing of the speed. Figure 10 presents actual flux $|\hat{\psi}_s|$ The estimated flux and $|\hat{\psi}_s|$ estimation error (er).

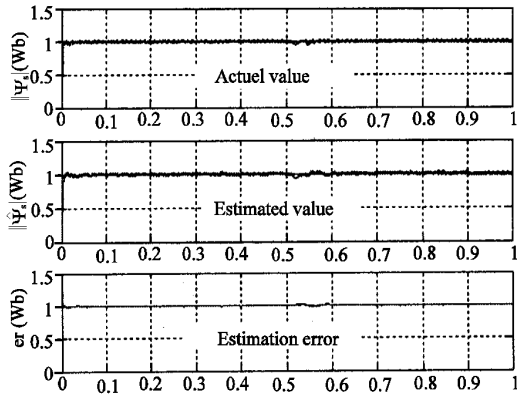


Fig. 10: The actual estimated stator flux magnitude and estimation error

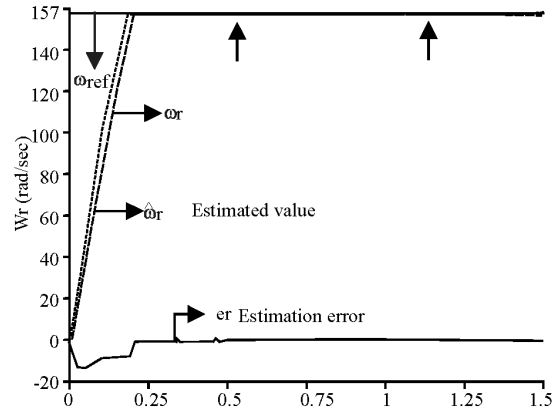


Fig. 12: High speed full-load speed estimation

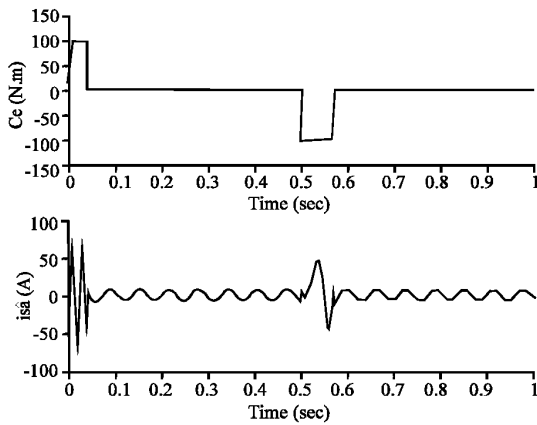


Fig. 11: Response of the electromagnetic torque and estimated stator current

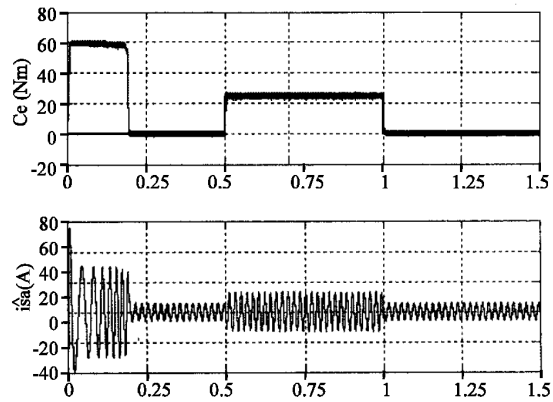


Fig. 13: Response of the electromagnetic torque and estimated stator current

Figure 11 illustrates the response of the estimated stator current and the electromagnetic torque. It should be noted that the amplitude of the torque ripple is slightly higher.

Variation of load torques: In Figure 12 and 13, rated mechanical load is applied to the motor between 0.5s-1s after a leadless starting. To verify the performance of EKF under loaded conditions. As shown above EKF works properly even under fully loaded case. We can see the insensibility of the control algorithm to load torque variation.

Injected noise to the stator currents: The aim of the current injection is to observe the low pass filter characteristics of EKF. As shown in Fig. 14, the estimated speed is not affected too much from the injected noise. The speed estimation accuracy may be increased by

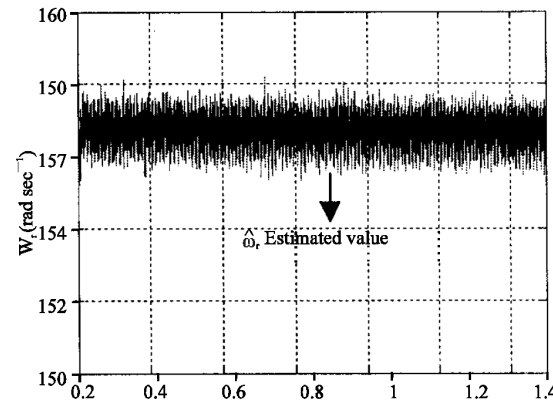


Fig. 14: Estimated rotor speed with measured noisy current

increasing the measurement noise covariance under noisy conditions thus; the system model will have more importance.

CONCLUSION

We have presented in this study sensorless direct torque control of induction motor based on Extended Kalman Filter for stator flux and speed estimation. The filtering action of EKF improves the system performance, especially at low speeds. Simulation results reveal that the flux and speed tracking are good and error convergence is guaranteed. However an anti-windup PI regulator has been used to replace the classical PI controller in the speed control of a direct torque control. In conclusion, it seems that the anti-windup PI controller outperforms the classical PI controller in speed control of high performance DTC motor drive. This association makes the induction motor based DTC more robust and more stable.

REFERENCES

- Akin, B., 2003. State estimation techniques for speed sensorless field oriented control of induction motors, M.Sc. Thesis EE Dept, METU.
- Barut, M., O. S. Bogosyan and M. Gokasan, 2003. An EKF based reduced order estimator for the sensorless control of IMs, IEEE., pp: 1256-1261.
- Barut, M., S. Bogosyan and M. Gokasan, 2005. EKF based sensorless direct torque control of IMs in the low speed range, IEEE Trans. Indus. Elec. ISIE, pp: 969-974.
- Belkacem, S., F. Naceri, A. Betta and L. Laggoune 2005. Speed sensorless DTC of induction motor based on an improved adaptive flux observer, IEEE. Trans. Indus. Applied Hong Kong, pp: 1192-1197.
- Belkacem, S., L. Louanasse, H. Tamrabet, S. Zaidi and B. Kiyyour, 2005. Performance Analysis of a Speed Sensorless Induction Motor Drive based on DTC scheme, First Int. Conf. Elec. Sys. PCSE, Oum El-Bouaghi, Algeria, pp: 267-272.
- Bottiglieri, G., G. Scelba and G. Scarcella, 2003. Sensorless speed estimation in induction motor drives, IEEE. Elec. Mac. IEMDC, pp: 624-630.
- Cao, Y., Z. Lin and D.G. Ward, 2002. An anti-windup approach to enlarging domain of attraction for linear systems subject to actuator saturation, IEEE. Trans. Automat Control, 47: 140-145.
- Chávez, S., R. Velázquez, Alejos Palomares and A. Nava Segura, 2004. Speed Estimation for an Induction Motor Using the Extended Kalman Filter, IEEE Transaction Electronics, Communications.
- Leite, A.V., R. E. Araujo and D. Freitas, 2004. Full and reduced order extended kalman filter for speed estimation in induction motor drives: A comparative study, Power Electronics Specialists Conference, PESC. IEEE., 3: 2293-2299.
- Leite, A.V., R. E. Araujo and D. A Freitas, 2004. New approach for speed estimation in induction motor drives based on a reduced-order extended Kalman filter, IEEE. Indus. Elec., pp: 1221-1226.
- Sensorless Control with Kalman Filter on TMS320 Fixed-Point DSP, Texas Instruments. Available: <http://www.ti.com>.
- Takahashi and T. Noguchi, 1986. A new quick-response and high efficiency control strategy of an induction machine, IEEE. Trans. Indus. Applied, 22: 820-827.
- Zaccarian, L. and A. Teel, 2004. Nonlinear scheduled anti-windup design for linear systems, IEEE. Trans. Automat Control, 49: 2055-2061.